Load Frequency Control in Power Systems via A Sampled-Data Controller

XingChen ShangGuan[1,2], Yong He[1,2], Lin Jiang[3]

1. School of Automation, China University of Geosciences, Wuhan 430074, P. R. China

2. Hubei Key Laboratory of Advanced Control and Intelligent Automation for Complex Systems, Wuhan 430074, P. R. China
E-mail: heyong08@cug.edu.cn (Yong He)

3. University of Liverpool, Brownlow Hill, Liverpool L69 3GJ, UK
E-mail: ljiang@liverpool.ac.uk (Lin Jiang)

Abstract: In modern power systems, load frequency control (LFC) scheme usually operates in the discrete mode, while the most existing LFC schemes are designed in the continuous mode, such that those LFC schemes do not work usually in their best manner in practice. In this paper, a method of state-feedback controller design of load frequency control (LFC) for one–area system is discussed in continuous-discrete mode via sampled–data control scheme. At first, the model of LFC is constructed in continuous-discrete mode by using the input delay method. Then, a new method is present to design a state–feedback controller. Finally, a case study is given to show the effectiveness and the benefits of the proposed method.

Key Words: Power system, Load frequency control, Sampled-data control, State–feedback controller

1 Introduction

With the rapid development of science, technology and e-conomy, people's demand of electricity is growing, which makes the power systems equip more and more renewable energy, such that the size of the power systems continues to expand [1]. When the system is subjected to the load fluctuation or disturbances, the operating point of the power system will change, and hence, system may experience deviations in nominal system frequency and scheduled power exchanges to other areas, which may degrade the performance of system and even yield power grid accident. In order to maintain the balance for the supply and demand of power, and thus to restore the frequency of the power systems to an acceptable range, load frequency control (LFC) was put forward to accomplish successfully power system operation [2]–[3].

The LFC is a significantly important means to regain the rated frequency within a few minutes after power system faults or disturbances [4]. Over the past few decades, a great attention has been paid to LFC. And a lot of control strategies have been applied in LFC, such as internal model control [5]–[6], sliding model control [7], optimal control [8], adaptive and self-tuning control [9], active disturbance rejection control [10], robust control [11], PI/PID control [12]–[13]. Almost all of those LFC controllers are designed based on the continuous mode. However, the practical controllers usually operate in the discrete mode with a sampling period of 2s–4s. So, above controllers do not work usually in their best manner in practice [14].

In practical power systems, open network control systems are commonly applied in LFC [16]. Such network control system (NCS) [15] is a system whose control loops are closed through a communication network such that both control signals and feedback signals can be exchanged among system components (sensors, controllers, and actuators). In a power system [16], control error signals are firstly sampled by sensors, then transmitted to controllers via zero order holders (ZOHs) and finally control signals are sent to actuators via ZOHs. This forms a discrete link structure of the sensor-controller-actuator (SCA), that is to say the power system can be regarded as a sampled-data control system of continuous-discrete.

During the last few decades, there have been some works introducing some controllers design for LFC via sampled-data strategy. In [17], a method of designing discrete-type load-frequency regulators was presented using discretized theory. Based on [17], a series of discrete-time controllers have been proposed in [18–20]. However, the design of such discrete-time controllers was only based on the directly discretized plant model with regarding sampling period as discretized period. It is worth mentioning that the control signal is updated almost every two seconds in power system [14]. When the discretized period is two seconds, it will be equivalent to the update period of control signal such that the Shannon sampling theorem cannot be satisfied [21]. This problem was well circumvented in [22], where Kanchanaharuthai designed a sampled-data controller and considered the intersample information using the technique of sampled-data system. Such technique has been well developed by Fridman et al. [23, 24], who introduce an input delay method to transform continuous-discrete sampled-data system into continuous time-delay system. Note that modern LFC system is a typical sampled-data system, but the input delay method has not been used in power system so far. Whats more, the communication delay was ignored during the above discrete-time controllers design. Therefore, there will be much room to be improved for designing a sampled-data controller.

According to the above discussions, this paper presents a method of state-feedback controller design of LFC via a sampled-data control scheme. Firstly, based on the input delay method, the model of LFC of power systems is established under the continuous-discrete structure. Then, the state-feedback controller is obtained by using a novel method. Finally, the accuracy of the obtained results is

1

shown by Simulink simulation.

The remainder of the paper is organized as follows. Section II gives the dynamic model of LFC for one–area power system. Section III proposes a controller solving method. In Section IV, a case study is given. Conclusion is given in Section V.

2 Dynamic Model of LFC

This section describes the model of LFC for one-area power system via state–feedback controller in traditional environment, which includes one control area. Such control area has a number of generators, and all generators are simplified as an equivalent generator unit [3]. The structure of one-area power system is shown in Fig. 1. To simplify the analysis, the time delays, including communication delays and fault-induced delays can be integrated into one single time delay and represented by an exponential block $e^{-s\tau}$ with $\tau \geq 0$, as shown in Fig. 1. For LFC scheme, the system of one–area power system can be obtained

$$\dot{\hat{x}}(t) = \hat{A}\hat{x}(t) + \hat{B}\hat{u}(t - \tau) + \hat{F}\hat{\omega}(t) \tag{1}$$

where

$$\hat{x}^T = [\Delta f \ \Delta P_m \ \Delta P_v] \ \hat{u}(t - \lambda) = \Delta P_c(t) \ \hat{\omega}(t) = \Delta P_d$$

$$\hat{A} = \begin{bmatrix} -\frac{D}{M} & \frac{1}{M} & 0 \\ 0 & -\frac{1}{T_{ch}} & \frac{1}{T_{ch}} \\ -\frac{1}{RT_g} & 0 & -\frac{1}{T_g} \end{bmatrix}$$

$$\hat{B} = \begin{bmatrix} 0_{1\times2} & \frac{1}{T_g} & 0 \end{bmatrix}^T \ \hat{F} = \begin{bmatrix} -\frac{1}{M} & 0_{1\times2} \end{bmatrix}^T$$

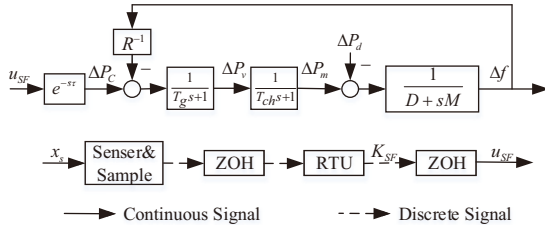and $\Delta f, \Delta P_m, \Delta P_v, \Delta P_d$ are the deviation of frequency,

Fig. 1: LFC Structure for one-area power system via state–feedback controller.

generator mechanical output, valve position, and load, respectively; M, D, T_g, T_ch, R represent the moment of inertia of generator unit, generator unit damping coefficient, time constant of the governor, time constant of the turbine, and speed droop, respectively; and τ represents the time delay.

In state feedback control, in order to force the steady state of Δf to tend to zero, the integral of Δf is used as an additional state, it is defined as

$$\Delta E = K_I \int \Delta f(t)dt \tag{2}$$

where K_I is the gain of integral controller.

Redefine the state vector as follows

$$x^T = \begin{bmatrix} \Delta f & \Delta P_m & \Delta P_v & \Delta E \end{bmatrix}$$

then the whole system is written as

$$\dot{x}(t) = Ax(t) + Bu(t - \tau) + F\omega(t) \tag{3}$$

where

$$A = \begin{bmatrix} -\frac{D}{M} & \frac{1}{M} & 0 & 0 \\ 0 & -\frac{1}{T_{ch}} & \frac{1}{T_{ch}} & 0 \\ -\frac{1}{RT_g} & 0 & -\frac{1}{T_g} & 0 \\ K_I & 0 & 0 & 0 \end{bmatrix}$$

$$B = \begin{bmatrix} 0_{1\times2} & \frac{1}{T_g} & 0 \end{bmatrix}^T \ F = \begin{bmatrix} -\frac{1}{M} & 0_{1\times3} \end{bmatrix}^T.$$

Based on Fig. 1, using $t_k, k = 0, 1, 2 \cdots$ as sampling time and $0 = t_0 < t_1 < \cdots < t_k$, and defining $t_{k+1} - t_k = h_k$ with sampling period $0 < h_k \leq h_M$, the state–feedback controller is designed as follow:

$$\begin{cases} u_{SF}(t_k) = K_{SF}x(t_k) \\ u(t - \tau) = u_{SF}(t_k - \tau) \end{cases} \quad t_k \leq t < t_{k+1} \tag{4}$$

where h_M represents the maximum sampling period (MSP).

By combining (3) and (4), the new closed-loop system can be derived as follow:

$$\dot{x}(t) = Ax(t) + BK_{SF}x(t_k - \tau) + F\omega(t) \atop t_k \leq t < t_{k+1} \tag{5}$$

Studying the balance point's inner stability of the system (5) is equivalent to analyse the origin's of the following system

$$\dot{x}(t) = Ax(t) + BK_{SF}x(t_k - \tau) \quad t_k \leq t < t_{k+1} \tag{6}$$

In this paper, the objective is aimed to design an effective method to derive the state–feedback controller via the sampled-data control scheme.

3 Main Results

In this section, an effective method is proposed to design a state-feedback controller. Given the LFC scheme for one–area in (6), the following result is developed.

Theorem 1. *For a given maximum sampling period, $h_M > 0$, and $\tau > 0$, if there exist symmetric matrices P, Q, $R \geq 0$, $Z \geq 0$ and $\bar{P} = \begin{bmatrix} P_1 + P_1^T & -P_1 - P_2 \\ * & P_2 + P_2^T \end{bmatrix}$, and any appropriately dimensioned matrices $M = [M_1^T \ M_2^T]^T$ and $L_j = [L_{1j}^T, L_{2j}^T, \cdots, L_{4j}^T]^T$, $j = 1, 2, \cdots, 4$, such that the following four LMIs hold:*

$$P > 0 \tag{7}$$

$$\begin{bmatrix} \Psi & -h_M M \\ * & Q \end{bmatrix} \geq 0 \tag{8}$$

$$\begin{bmatrix} \Xi_1 + h_M\Xi_2 & -L_3 & -\sqrt{\tau}L_2 & -\sqrt{h_M}L_3 \\ * & -R & 0 & 0 \\ * & * & -Z & 0 \\ * & * & * & -Z \end{bmatrix} \leq 0 \tag{9}$$

$$\begin{bmatrix} \Xi_1 & -L_3 & -\sqrt{h_M}L_1 & -\sqrt{\tau}L_2 \\ * & -R & 0 & 0 \\ * & * & -(Z + Q) & 0 \\ * & * & * & -Z \end{bmatrix} \leq 0 \tag{10}$$

2

where

$$\Psi = \mathrm{diag}\{P, 0\} + h_M(\bar{P} + ME + E^T M^T)$$

$$\Xi_1 = \begin{bmatrix} R - P_1 - P_1^T & P_1 + P_2 & 0 & P \\ * & -P_2 - P_2^T & 0 & 0 \\ * & * & 0 & 0 \\ * & * & * & \eta Z \end{bmatrix}$$

$$+ \sum_{i=1}^{4}(L_i E_i + E_i^T L_i)$$

$$\Xi_2 = \begin{bmatrix} 0 & 0 & 0 & P_1 + P_1^T \\ * & 0 & 0 & -P_1^T - P_2^T \\ * & * & 0 & 0 \\ * & * & * & Q \end{bmatrix}$$

$$E = [I, \ -I], \ E_1 = [I \ -I \ 0 \ 0], \ E_2 = [0 \ I \ -I \ 0],$$
$$E_3 = [0 \ 0 \ I \ 0], \ E_4 = [-A \ 0 \ -BK_{SF} \ I]$$

then the closed-loop system (6) with a variable sampling period h, satisfying $h \leq h_M$, is asymptotically stable. And, $P > 0 \ (\geq 0)$ means that P is a real symmetric and positive-definite (semi-positive-definite) matrix; I and 0 represent the identity matrix and a zero matrix, respectively; the superscript T represents the transpose; $\mathrm{diag}\{\cdots\}$ stands for a block-diagonal matrix; the notation $*$ always denotes the symmetric block in a symmetric matrix.

Proof. For the one–area system (6), the following candidate LKF is introduced

$$V(x_t) = \sum_{i=1}^{3} V_i(x_t), t \in [t_k, t_{k+1}) \tag{11}$$

with

$$V_1(x_t) = x^T(t)Px(t) + (h_k - d_k(t))\varepsilon_1^T(t)\bar{P}\varepsilon_1(t)$$
$$+ (h_k - d_k(t)) \int_{t-d_k(t)}^{t} \dot{x}^T(s)Q\dot{x}(s)\mathrm{d}s$$

$$V_2(x_t) = 2(h_k - d_k(t))\varepsilon_1^T(t)M$$
$$\times \left[x(t) - x(t - d_k(t)) - \int_{t-d_k(t)}^{t} \dot{x}(s)\mathrm{d}s \right]$$
$$= (h_k - d_k(t))\varepsilon_2^T(t)\left[\bar{M}^T + \bar{M}\right]\varepsilon_2(t)$$

$$V_3(x_t) = \int_{t-\eta_k}^{t} x^T(s)Rx(s)\mathrm{d}s$$
$$+ \int_{-\eta_k}^{0}\int_{t+\theta}^{t} \dot{x}^T(s)Z\dot{x}(s)\mathrm{d}s\mathrm{d}\theta$$

where

$$d_k(t) = t - t_k \quad \eta_k = h_k + \lambda$$
$$\varepsilon_1(t) = \begin{bmatrix} x(t) \\ x(t - d_k(t)) \end{bmatrix}$$
$$\varepsilon_2(t) = \begin{bmatrix} \varepsilon_1(t) \\ \int_{t-d_k(t)}^{t} \dot{x}(s)\mathrm{d}s \end{bmatrix}$$
$$\bar{P} = \begin{bmatrix} P_1 + P_1^T & -P_1 - P_2 \\ * & P_2 + P_2^T \end{bmatrix}$$
$$\bar{M} = \begin{bmatrix} M & -M & -M \\ 0 & 0 & 0 \end{bmatrix} \quad M = \begin{bmatrix} M_1 \\ M_2 \end{bmatrix}.$$

Based on the proposed method of [24], for such LKF, the following conditions can achieve the system (6) asymptotically stable

$$\begin{cases} V(x_t) \geq 0 \\ \lim_{t \to t_k^-} V(x_t) \geq V(x_t)|_{t=t_k^+} \\ \dot{V}(x_t) < 0 \end{cases} \tag{12}$$

Firstly, from the above LKF, it is easy to obtain that

$$\lim_{t \to t_k^-} V(x_t) \geq V(x_t)|_{t=t_k^+} \tag{13}$$

Secondly, rewriting the $V_1(x_t) + V_2(x_t)$ by splitting $V_2(x_t)$ yields

$$V_1(x_t) + V_2(x_t)$$
$$= \frac{d_k(t)}{h_k}x^T(t)Px(t) + \frac{h_k - d_k(t)}{h_k}\varepsilon_1^T(t)\Psi\varepsilon_1(t)$$
$$+ \frac{h_k - d_k(t)}{h_k}\int_{t-d_k(t)}^{t} \begin{bmatrix} \varepsilon_1(t) \\ \dot{x}(s) \end{bmatrix}^T \begin{bmatrix} 0 & -h_k M \\ & h_k Q \end{bmatrix}$$
$$\times \begin{bmatrix} \varepsilon_1(t) \\ \dot{x}(s) \end{bmatrix}\mathrm{d}s$$
$$\geq \frac{d_k(t)}{h_k}x^T(t)Px(t) + \frac{h_k - d_k(t)}{h_k^2}$$
$$\times \int_{t-d_k(t)}^{t} \begin{bmatrix} \varepsilon_1(t) \\ \dot{x}(s) \end{bmatrix}^T \begin{bmatrix} \Psi & -h_k^2 M \\ * & h_k^2 Q \end{bmatrix} \begin{bmatrix} \varepsilon_1(t) \\ \dot{x}(s) \end{bmatrix}\mathrm{d}s$$

By using Schur complement, $\begin{bmatrix} \Psi & -h_k M \\ * & Q \end{bmatrix} \geq 0$ is equivalent to $\begin{bmatrix} \Psi & -h_k^2 M \\ * & h_k^2 Q \end{bmatrix} \geq 0$. Therefore, $V(x_t) \geq 0$ when $R \geq 0$, $Z \geq 0$ and LMIs (7) and (8) hold.

Thirdly, evaluating the derivative of the LKF. Using the Newton-Leibnitz formula, for any appropriately dimensioned matrices $L_j, j = 1, 2, \cdots, 4$, the following equations are true:

$$0 = 2\varepsilon^T(t)L_1[x(t) - x(t - d_k(t)) - d_k(t)v_1(t)]$$
$$0 = 2\varepsilon^T(t)L_2[x(t - d_k(t)) - x(t - \bar{d}_k(t)) - \tau v_2(t)]$$
$$0 = 2\varepsilon^T(t)L_3$$
$$\times [x(t - \bar{d}_k(t)) - x(t - \eta_k) - (h_k - d_k(t))v_3(t)]$$
$$0 = 2\varepsilon^T(t)L_4[\dot{x}(t) - Ax(t) - BK_{SF}x(t - \bar{d}_k(t))]$$

where

$$v_1(t) = \frac{1}{d_k(t)}\int_{t-d_k(t)}^{t} \dot{x}(s)\mathrm{d}s$$
$$v_2(t) = \frac{1}{\tau}\int_{t-\bar{d}_k(t)}^{t-d_k(t)} \dot{x}(s)\mathrm{d}s$$
$$v_3(t) = \frac{1}{h_k - d_k(t)}\int_{t-\eta_k(t)}^{t-\bar{d}_k(t)} \dot{x}(s)\mathrm{d}s$$
$$\bar{d}_k(t) = d_k(t) + \tau$$
$$\varepsilon(t) = [x^T(t) \ x^T(t - d_k(t)) \ x^T(t - \bar{d}_k(t)) \ \dot{x}^T(t)]^T.$$

Then, differentiating $V(x_t)$ with considering of (6) for $t_k < t < t_{k+1}$, using Jensen inequality [25] to process

3

Q and Z integral-term-derivative and applying above zero-equations yield

$$V(x_t) = \frac{h_k - d_k(t)}{h_k} \xi_1^T(t) \Xi_a \xi_1(t) + \frac{d_k(t)}{h_k} \xi_2^T(t) \Xi_b \xi_2(t)$$

where

$$\xi_1(t) = \begin{bmatrix} \varepsilon(t) \\ x(t - \eta_k) \\ v_2(t) \\ v_3(t) \end{bmatrix}, \xi_2(t) = \begin{bmatrix} \varepsilon(t) \\ x(t - \eta_k) \\ v_1(t) \\ v_2(t) \end{bmatrix}$$

$$\Xi_a = \begin{bmatrix} \Xi_1 + h_k \Xi_2 & -L_3 & -\tau L_2 & -h_k L_3 \\ * & -R & 0 & 0 \\ * & * & -\tau Z & 0 \\ * & * & * & -h_k Z \end{bmatrix}$$

$$\Xi_b = \begin{bmatrix} \Xi_1 & -L_3 & -h_k L_1 & -\tau L_2 \\ * & -R & 0 & 0 \\ * & * & -h_k(Z + Q) & 0 \\ * & * & * & -\tau Z \end{bmatrix}$$

Obviously, it is easy to check that $\Xi_a \leq 0$ and $\Xi_b \leq 0$ are convex in h_k, then LMIs (9) and (10) lead to $\Xi_a \leq 0$ and $\Xi_b \leq 0$, respectively.

Combining the above analysis, it is able to prove that conditions (12) hold to accomplish the asymptotical stability of the closed-loop system. The proof is completed. □

Remark 1. *The LMIs of Theorem 1 are affine in the system matrices and it can be used to deal with the system with poly-type uncertainty. Moreover, as mentioned in [26], the exponential stability of system can be directly analyzed based on the asymptotical stability criterion by rewriting the original system as a new system with polytype uncertainty, i.e., representing system (6) as*

$$\dot{\bar{x}}(t) = \sum_{i=1}^{2} \mu_i(t) \left[(A + \lambda I) \bar{x}(t) + \rho_i B K_{SF} \bar{x}(t_k - \tau) \right]$$

where

$$\mu_1(t) = \frac{\rho_2 - e^{\lambda \bar{d}(t)}}{\rho_2 - \rho_1} \quad \mu_2(t) = \frac{e^{\lambda \bar{d}(t)} - \rho_1}{\rho_2 - \rho_1}$$

$$\rho_1 = e^{\lambda \tau} \quad \rho_2 = e^{\lambda(\tau + h_M)}.$$

Considering the LMIs of Theorem 1, due to the uncoupled relationship between the matrices in the LKF and the system matrices, this theorem can be easily extended to system stabilization.

Theorem 2. *For a preset h_M and τ, and the given parameters a, b and c, the closed-loop system (6) is asymptotically stable and the control gain can be obtained by $K_{SF} = V\hat{S}^{-T}$, if the following condition is satisfied: there exist symmetric matrices $\hat{P} > 0$, $\hat{Q}$, $\hat{R} \geq 0$, $\hat{Z} \geq 0$ and $\hat{\bar{P}} = \begin{bmatrix} \hat{P}_1 + \hat{P}_1^T & -\hat{P}_1 - \hat{P}_2 \\ * & \hat{P}_2 + \hat{P}_2^T \end{bmatrix}$, and any appropriately dimensioned matrices $\hat{M} = [\hat{M}_1^T \quad \hat{M}_2^T]^T$, $\hat{L}_j = [\hat{L}_{1j}^T, \hat{L}_{2j}^T, \cdots, \hat{L}_{4j}^T]^T$, $j = 1, 2, 3$, $\hat{S}$, and V such that the following LMIs hold:*

$$\begin{bmatrix} \hat{\Psi} & -h_M \hat{M} \\ * & \hat{Q} \end{bmatrix} \geq 0 \tag{14}$$

$$\begin{bmatrix} \Pi & -\hat{L}_3 & -\sqrt{\tau}\hat{L}_2 & -\sqrt{h_M}\hat{L}_3 \\ * & -\hat{R} & 0 & 0 \\ * & * & -\hat{Z} & 0 \\ * & * & * & -\hat{Z} \end{bmatrix} \leq 0 \tag{15}$$

$$\begin{bmatrix} \hat{\Xi}_1 & -\hat{L}_3 & -\sqrt{h_M}\hat{L}_1 & -\sqrt{\tau}\hat{L}_2 \\ * & -\hat{R} & 0 & 0 \\ * & * & -(\hat{Z} + \hat{Q}) & 0 \\ * & * & * & -\hat{Z} \end{bmatrix} \leq 0 \tag{16}$$

where

$$\Pi = \hat{\Xi}_1 + h_M \hat{\Xi}_2$$

$$\hat{\Xi}_1 = \begin{bmatrix} \hat{R} - \hat{P}_1 - \hat{P}_1^T & \hat{P}_1 + \hat{P}_2 & 0 & \hat{P} \\ * & -\hat{P}_2 - \hat{P}_2^T & 0 & 0 \\ * & * & 0 & 0 \\ * & * & * & \eta\hat{Z} \end{bmatrix}$$

$$+ \sum_{i=1}^{3} \left(\hat{L}_i E_i + E_i^T \hat{L}_i \right) + E_5^T \hat{E}_4 + \hat{E}_4^T E_5$$

$$\hat{\Xi}_2 = \begin{bmatrix} 0 & 0 & 0 & \hat{P}_1 + \hat{P}_1^T \\ * & 0 & 0 & -\hat{P}_1^T - \hat{P}_2^T \\ * & * & 0 & 0 \\ * & * & * & \hat{Q} \end{bmatrix}$$

$$E_1 = [I \ -I \ 0 \ 0] \quad E_2 = [0 \ I \ -I \ 0] \quad E_3 = [0 \ 0 \ I \ 0]$$

$$\hat{E}_4 = \begin{bmatrix} -A\hat{S}^T \ 0 \ -BV \ \hat{S} \end{bmatrix} \quad E_5 = [I \ aI \ bI \ cI].$$

Proof. Denote $S_2 = aS_1$, $S_3 = bS_1$, $S_4 = cS_1$ (where a, b and c are scalars), $\hat{S} = S_1^{-1}$, $\hat{P} = \hat{S}P\hat{S}^T$, $\hat{Q} = \hat{S}Q\hat{S}^T$, $\hat{P}_i = \hat{S}P_i\hat{S}^T$, $\hat{M}_i = \hat{S}M_i\hat{S}^T$, $\hat{L}_j = \hat{S}L_j\hat{S}^T$, $j = 1, 2, 3$, and $V = K_{SF}\hat{S}^T$. Pre- and post-multiply (7) by $\hat{S}$ and $\hat{S}^T$, pre- and post-multiply (8) by diag$\{\hat{S}, \hat{S}, \hat{S}\}$ and diag$\{\hat{S}^T, \hat{S}^T, \hat{S}^T\}$, and pre- and post-multiply (9) and (10) by diag$\{\hat{S}, \hat{S}, \hat{S}, \hat{S}\}$ and diag$\{\hat{S}^T, \hat{S}^T, \hat{S}^T, \hat{S}^T\}$, then the above theorem is obtained. □

Remark 2. *The controller gains obtained using Theorem 2 is dependent on parameters a, b and c tuned by the designer. Combining Remark 1, decay rate λ is introduced into the design of controllers, and it can be regarded as the dynamic speed performance index to evaluate the quality of controller. The corresponding controller gains can be obtained based on Remark 1 and Theorem 2.*

Detailed procedure of the proposed method is summarized as the following steps.

Step 1) Obtain the state-space model of the closed-loop LFC scheme for one-area power system and transform it into a system providing with a state-feedback controller, as introduced in Section II.

Step 2) Controller design. For given system parameters, the sampling period h, the time delay τ and the decay rate λ, the feasible controller K_{SF} can be derived by combining Theorem 2 and Remark 1 to realize the exponential stability of system (6).

Step 3) Performance analysis. Based on Theorem 1 and Remark 1, for given system parameters, the controller K_{SF}, the sampling period h, the time delay τ, the system dynamic speed performance can be accessed by maximizing the decay rate λ.

Step 4) Simulation verification. Simulation studies are carried out to verify the effectiveness of the method proposed.

4 Case Studies

The simulation case is based on LFC scheme of one-area power system with state-feedback controller. It is assumed that such area contains one Genco and one Disco and the relevant parameters shown in Table 1. Controller design and system dynamic speed performance analysis are presented for this system. In order to illustrate some existing controllers do not work usually in their best manner in practice and show the effectiveness of our method proposed, based on Theorem 1, we calculate the maximum sampling periods (MSPs) of four existing state-feedback controllers, as described in [27]. The simulation studies are completed on the Simulink models based on Fig. 1 Based on Theorem 2 and

Table 1: Parameters of System

	M	D	R	T_{ch}	T_g	K_I
Value	1/6	1/120	2.4	0.3	0.08	1

Remark 1, by setting the time delay $\tau = 1s$, $h_M = 2s$ and choosing $a = b = 0$ and $c = 4.63$, the controller gains is obtained by maximizing λ as

$$K_1 = -[0.0311 \;\; 0.0617 \;\; 0.0110 \;\; 0.2031] \qquad (17)$$

and $\lambda_M = 0.2531$.

By using the method given in Theorem 1 and Remark 1, The maximal exponential decay rate (MEDR) of the closed-loop system for controller K_1 for different constant time delays and sampling periods are calculated and listed in Table 2. Table 2 shows that the value of the MEDRs decreases with

Table 2: MEDRs for different sampling periods and time delays

| h | | τ | | |
	0.5	1	1.5	2
1	0.53	0.40	0.32	0.27
2	0.31	0.25	0.21	0.19
3	0.21	0.19	0.15	0.14
4	0.15	0.14	0.14	0.12

the increasing of the time delays or sampling periods. Moreover, the largest MEDR is 0.53 when $h = 1$ and $\tau = 0.5$, while the MEDR is lowest at 0.12 when $h = 4$ and $\tau = 2$.

Four state-feedback controllers given in [27] (named as $K_2 \sim K_5$) and K_1 in this paper and the corresponding MSPs calculated based on Theorem 1 (named as $\mathrm{MSP_T}$) and simulation studies (named as $\mathrm{MSP_S}$) are listed in Table 3 by setting $\tau = 0$. The calculated values are closed to the ones obtained by simulation studies, which shows the accuracy of the proposed criterion. It is easy to see that controllers $K_2 \sim K_5$ cannot be used in practice because their MSPs are much smaller than the commonly used sampling period of

2s. Compared with controllers $K_2 \sim K_5$, the MSP of K_1 can reach 4.5s more than double 2s. So, our controller is superior to controllers $K_2 \sim K_5$.

Table 3: Controllers $K_1 \sim K_5$ and the corresponding MSP

Controller	$\mathrm{MSP_T}$ (s)	$\mathrm{MSP_S}$ (s)
K_1 [in this paper]	4.50	4.65
K_2=-[1.893 4.762 1.516 1.658]	0.10	0.11
K_3=-[5.030 8.726 2.132 1.625]	0.07	0.07
K_4=-[2.732 4.017 0.851 0.432]	0.17	0.17
K_5=-[13.738 16.077 2.837 19.118]	0.05	0.05

The resulting closed-loop system is simulated in presence of a 0.1 per unit step load demand at 0.5 s. For time delay $\tau = 0$ and sampling period $h = 2s$, the response sof frequency deviation are shown in Fig. 2, where the results provided by controllers $K_2 \sim K_5$ are also given for comparison. This figure shows that the controller K_1 obtained by the proposed method can work well in discrete mode with the preset sampling period $h = 2s$ and make the frequency deviation converge to 0 within the desired time. For time delay $\tau = 1s$, the responses of frequency deviation are displayed in Fig. 3 for differen sampling periods. From Fig. 3, it can be seen that the controller K_1 obtained by the proposed method can generate effective actions to achieve the system stable, regardless of $h = 1s$, $2s$ or $4s$, which shows that our controller can work well in practical LFC, though time delays exist in LFC.
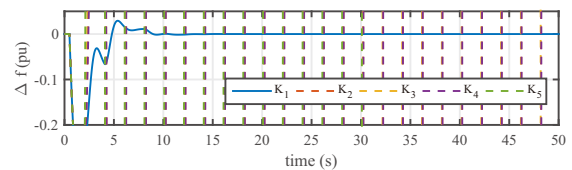

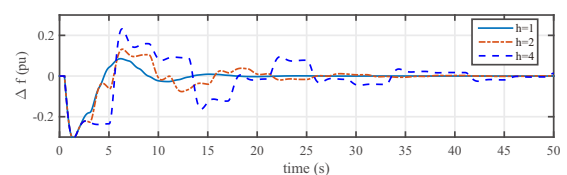Fig. 2: The responses of frequency deviation for $\tau = 0$.

Fig. 3: The responses of frequency deviation for $\tau = 1s$.

5 Conclusion

In this paper, the problem that controller is designed in discrete mode has been discussed. Firstly, the model of LFC for one–area power system providing state–feedback controller has been built via sampled-data control scheme. Secondly, based on the model, an effective method has been proposed to design a state–feedback controller and the controller gains have been calculated by using the system stability condition. Finally, the accuracy of the obtained result has been demonstrated via simulation case.

References

[1] J. Momoh. *Smart Grid: Fundamentals of Design and Analysis*, Wiley, 2012.

[2] L. K. Kirchmayer. Tie-line power and frequency control of electric power systems, *IEEE Transactions on Power Apparatus and Systems* 1953; 72(2): 562-572.

[3] P. Kundur. *Power System Stability and Control*, New York: Mc-Graw-Hill, 1994.

[4] Ibraheem, P. Kumar, and D. P. Kothari. Recent philosophies of automatic generation control strategies in power systems. *IEEE Transactions on Power Systems* 2005; 20(1): 346-357.

[5] A. Petersson , L. Harnefors , and T. Thiringer. Evaluation of current control methods for wind turbines using doubly-fed induction machines, *IEEE Transactions on Power Electronics* 2005; 20(1): 227-235.

[6] S. Saxena and Y. V. Hote. Load frequency control in power systems via internal model control scheme and model-order reduction, *IEEE Transactions on Power Systems* 2013; 28(3): 2749-2757.

[7] Y. Mi, Y. Fu, C. S. Wang, and P. Wang. Decentralized sliding mode load frequency control for multi-area power systems, *IEEE Transactions on Power Systems* 2013; 28(4): 4301-4309.

[8] R. K. Cavin, M. C. Budge, and P. Rasmussen. An optimal linear systems approach to load-frequency control, *IEEE Transactions on Power Apparatus and Systems* 1971; 90(6): 2472-2482.

[9] C. T. Pan, and C. M. Liaw. An adaptive controller for power system load-frequency control, *IEEE Power Engineering Review* 1989; 4(1): 122-128.

[10] F. Liu, Y. Li, Y. Cao, and J. H. She. A two-layer active disturbance rejection controller design for load frequency control of interconnected power system, *IEEE Transactions on Power Systems* 2016; 31(4): 3320-3321.

[11] G. Ray, A. N. Prasad, and G. D. Prasad. A new approach to the design of robust load-frequency controller for large scale power systems, *Electric Power Systems Research* 1999; 51(1): 13-22.

[12] Y. H. Moon, H. S. Ryu, J. G. Lee, and S. Kim. Power system load frequency control using noise-tolerable PID feedback, *IEEE International Symposium on Industrial Electronics* 2001; 3: 1714-1718.

[13] C. K. Zhang, L. Jiang, Q. H. Wu, Y. He, and M. Wu. Further results on delay-dependent stability of multi-area load frequency control, *IEEE Transactions on Power Systems* 2013; 28(4): 4465-4474.

[14] J. Nanda, A. Mangla, and S. Suri. Some new findings on automatic generation control of an interconnected hydrothermal system with conventional controllers, *IEEE Transactions on Energy Conversion* 2006; 21(1): 187-184.

[15] X. M. Zhang, Q. L. Han, and X. Yu. Survey on recent advances in networked control systems, *IEEE Transactions on Industrial Informatics* 2016; 12(5): 1740-1752.

[16] Y. Zhang, D. Yue, and S. Hu. Digital PID based load frequency control through open communication networks, *Chinese Control and Decision Conference* 2015; 6243-6248.

[17] T. Hiyama. Optimisation of discrete-type load-frequency regulators considering generation-rate constraints,*IEE Proceedings C Generation, Transmission and Distribution* 1982; 129(6): 285.

[18] J. S. Lim and Y. I. Lee. Design of discrete-time multivariable PID controllers via LMI approach, *International Conference on Control* 2008; 38(3): 1867-1871.

[19] K. Vrdoljak, I. Petrovic and N. Peric. Discrete-time sliding mode control of load frequency in power systems with input delay, *International Power Electronics and Motion Control Conference* 2006; 567-572.

[20] Y. Zhang and D. Yue. Digital PID based load frequency control through open communication networks, *IEEE Control and Decision Conference* 2015; 6243-6248.

[21] A. Kumar and O. P. Malik. Discrete analysis of load-frequency control problem, *IEE Proceedings C Generation, Transmission and Distribution* 1984; 131(4): 144-145.

[22] A. Kanchanaharuthai. Optimal sampled-data controller design with time-multiplied performance index for load-frequency control, *IEEE International Conference on Control Applications* 2004; 1:655-660.

[23] E. Fridman, A. Seuret, and J. P. Richard. Robust sampled-data stabilization of linear systems: An input delay approach, *Automatica* 2004; 40(8): 1441-1446.

[24] E. Fridman. A refined input delay approach to sampled-data control, *Automatica* 2010; 46(2): 421-427.

[25] K. Gu, V. Kharitonov, and J. Chen. *Stability of Time-delay Systems*, Boston: Birkhauser, 2003.

[26] K. Liu and E. Fridman. Wirtinger's inequality and Lyapunov-based sampled-data stabilization, *Automatica* 2012; 48(1): 102-108.

[27] W. Tan and Z. Xu. Robust analysis and design of load frequency controller for power systems, *Electric Power Systems Research* 2009; 79(5): 846-853.